The Guanine Cation Radical: Investigation of Deprotonation States by ESR and DFT

Amitava Adhikary,† Anil Kumar, David Becker, and Michael D. Sevilla*

Department of Chemistry, Oakland University, Rochester, Michigan 48309

Received: July 11, 2006; In Final Form: September 12, 2006

This work reports ESR studies that identify the favored site of deprotonation of the guanine cation radical ($G^{\bullet+}$) in an aqueous medium at 77 K. Using ESR and UV−visible spectroscopy, one-electron oxidized guanine is investigated in frozen aqueous D_2O solutions of 2′-deoxyguanosine (dGuo) at low temperatures at various pHs at which the guanine cation radical, $G^{\bullet+}$ (pH 3−5), singly deprotonated species, $G(-H)^{\bullet}$ (pH 7−9), and doubly deprotonated species, $G(-2H)^{\bullet-}$ (pH > 11), are found. C-8-deuteration of dGuo to give 8-D-dGuo removes the major proton hyperfine coupling at C-8. This isolates the anisotropic nitrogen couplings for each of the three species and aids our analyses. These anisotropic nitrogen couplings were assigned to specific nitrogen sites by use of ^{15}N-substituted derivatives at N1, N2, and N3 atoms in dGuo. Both ESR and UV−visible spectra are reported for each of the species: $G^{\bullet+}$, $G(-H)^{\bullet}$, and $G(-2H)^{\bullet-}$. The experimental anisotropic ESR hyperfine couplings are compared to those obtained from DFT calculations for the various tautomers of $G(-H)^{\bullet}$. Using the B3LYP/6-31G(d) method, the geometries and energies of $G^{\bullet+}$ and its singly deprotonated state in its two tautomeric forms, $G(N1-H)^{\bullet}$ and $G(N2-H)^{\bullet}$, were investigated. In a nonhydrated state, $G(N2-H)^{\bullet}$ is found to be more stable than $G(N1-H)^{\bullet}$, but on hydration with seven water molecules $G(N1-H)^{\bullet}$ is found to be more stable than $G(N2-H)^{\bullet}$. The theoretically calculated hyperfine coupling constants (HFCCs) of $G^{\bullet+}$, $G(N1-H)^{\bullet}$, and $G(-2H)^{\bullet-}$ match the experimentally observed HFCCs best on hydration with seven or more waters. For $G(-2H)^{\bullet-}$, the hyperfine coupling constant (HFCC) at the exocyclic nitrogen atom (N2) is especially sensitive to the number of hydrating water molecules; good agreement with experiment is not obtained until nine or 10 waters of hydration are included.

Introduction

ESR studies on γ-irradiated DNA or DNA-model structures[1,2] have shown that, at low temperatures, cytosine and thymine are the sites of electron gain, whereas guanine is the site of hole localization (electron loss). This result is in agreement with the electron affinities (EA) and the ionization potentials (IP) of the bases[3] as well as gas-phase and aqueous solution redox potential data.[4] Both the stabilization of the guanine cation radical ($G^{\bullet+}$) and the rate of subsequent hole transfer from $G^{\bullet+}$ to hole-acceptor sites has been shown to depend on prototropic equilibria (as shown in Scheme 1).[1f,4b,5]

Although much work has been performed on the guanine cation radical, the specific site of deprotonation is still an open question.[4a,b,5−7] Pulse radiolysis studies with both conductometric and optical detection have shown that, in aqueous solutions, 2′-deoxyguanosine (dGuo) is a good Brønsted acid with a pK_a of 3.9.[1,4−7] Pulse radiolysis studies also suggest that deprotonation of $G^{\bullet+}$ in dGuo occurs by loss of a proton from N1 to give $G(N1-H)^{\bullet}$ (Scheme 1).[5] At high pH, $G(N1-H)^{\bullet}$ further deprotonates to produce $G(-2H)^{\bullet-}$ (Scheme 1) with pK_a = 10.8.[5] It has also been shown that, for 5′-dGMP, the presence of the phosphate group does not affect this prototropic equilibria significantly.[4b] We note that the pK_a of the 1-methylguanosine cationic radical (1-Me-Guo$^{\bullet+}$) is 4.7,[5] which suggests that, in dGuo, deprotonation from the exocyclic nitrogen (N2) is competitive with deprotonation from N1 (Scheme 1). Theoretical calculations support this and show that the energies involved in producing the N1 deprotonated $G^{\bullet+}$, i.e., $G(N1-H)^{\bullet}$, or the N2 deprotonated $G^{\bullet+}$, i.e., $G(N2-H)^{\bullet}$, are very similar.[6] It has been proposed that $G(N1-H)^{\bullet}$ would be favored over $G(N2-H)^{\bullet}$ in environments with high dielectric constants, such as water.[6e]

ENDOR studies carried out using X-ray-irradiated single crystals of Guo, dGuo, 5′-dGMP, and 3′,5′-cyclic guanosine monophosphate show that $G(N2-H)^{\bullet}$ rather than $G(N1-H)^{\bullet}$ is formed via deprotonation of $G^{\bullet+}$.[7a−d,f,g,i,j,l] An earlier ENDOR study on X-ray-irradiated single crystals of 5′-dGMP that suggested $G(N1-H)^{\bullet}$ was formed[7e] has been questioned.[7b,] An ESR study in aqueous solution and the associated theoretical calculations[7k] suggested that, in $G^{\bullet+}$, the site of deprotonation is likely at N1; however, there are no definitive experimental results that show this.

In our laboratory, $G^{\bullet+}$ is produced by one-electron oxidation of dGuo and analogues by $Cl_2^{\bullet-}$ in an aqueous glass (7.5 M LiCl in D_2O).[8] Deuteration at C-8 in dGuo reduces the ca. 8 G anisotropic proton hyperfine coupling to a 1.2 G deuteron coupling and thereby narrows the line widths and improves resolution.[8b,9] Also, we have employed dGuo derivatives having ^{15}N substitution at N2 in dGuo ([2-^{15}N]-dGuo), at N1 and at N2 in dGuo ([1,2-^{15}N]-dGuo), and at N1, N2, and N3 in dGuo ([1,2,3-^{15}N]-dGuo) to verify both the values of the anisotropic N-couplings and the specific sites of those couplings in one-electron oxidized dGuo at various pHs. D_2O solutions are employed throughout the ESR experiments as they reduce line widths and improve resolution, relative to H_2O, by reducing the magnitude of hydrogen couplings for exchangeable hydrogen atoms. Using ESR spectroscopy and theoretical calculations,

* Corresponding author. E-mail: sevilla@oakland.edu. Telephone: 001 248 370 2328. Fax: 001 248 370 2321.

† On leave from Department of Chemistry, Rajdhani College, University of Delhi, Raja Garden, Delhi 110 015, India.

10.1021/jp064361y CCC: $33.50
Published on Web 11/04/2006

SCHEME 1: Prototropic Equilibria of One-Electron Oxidized Guanine Including the Cation Radical ($G^{\bullet+}$), the Monodeprotonated Species, G(N1−H)• and G(N2−H)•, in Syn- and Anti-conformers with Respect to the N3 Atom and the Dideprotonated Species, $G(-2H)^{\bullet-}$)

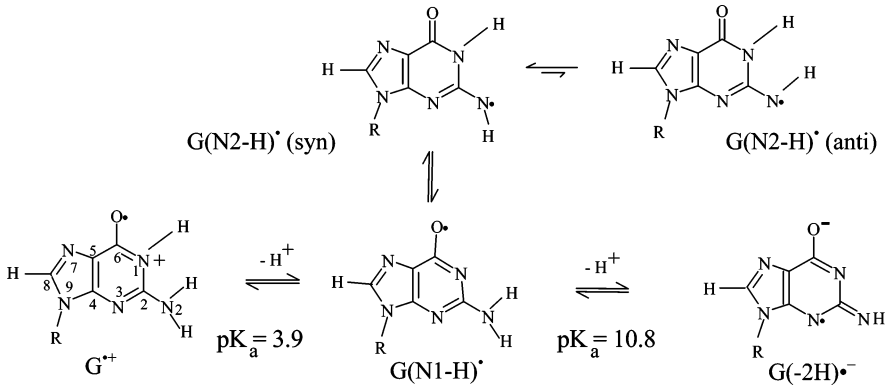

The numbering scheme shown here is followed in this work.

including water molecules as the hydration shell, we are able to identify the preferred site of deprotonation in $G^{\bullet+}$ in this aqueous system. To the best of our knowledge, our analyses of the ESR spectrum of dideprotonated $G^{\bullet+}$ (i.e., $G(-2H)^{\bullet-}$, Scheme 1) is the first in the literature.

Materials and Methods

Compounds Used. 2′-Deoxyguanosine (dGuo) and lithium chloride (99% anhydrous, SigmaUltra) were obtained from Sigma Chemical Company (St. Louis, MO). Potassium persulfate (crystal) was purchased from Mallinckrodt, Inc. (Paris, KY). We have carried out deuteration at C-8 in the guanine moiety of dGuo according to Huang et al.[8b−10] using triethylamine (TEA) from Fischer Scientific, NJ. The degree of deuteration (≥96%) was determined by 1D NMR signal integration employing a Bruker 200 MHz NMR.[8b] [2-^{15}N]-dGuo, [1,2-^{15}N]-dGuo, and [1,2,3-^{15}N]-dGuo were gifts from Prof. Roger Jones (Rutgers University, NJ).

Sample Preparation. About 3 mg of dGuo, its ^{15}N-substituted derivatives, or 8-D-dGuo was dissolved in 1 mL of 7.5 M LiCl in D_2O in the presence of 5 mg $K_2S_2O_8$ for preparation of the glassy samples. If required, the pH was adjusted under ice-cooled conditions by adding the appropriate μL amounts of 1 M NaOH in D_2O or concentrated HCl followed by mixing, and the samples were prepared quickly.[8b] pH papers were used for measurements of pH. Note "pH" is determined for D_2O solutions. Because of this and because of the high ionic strength of the glasses, the pH values reported here are approximations.[8b] The solutions were then thoroughly bubbled with nitrogen. Using these solutions, the glassy samples were then prepared by cooling to 77 K as reported earlier.[8] All samples are stored at 77 K.[8]

γ-Irradiation. As in our earlier works,[8] the glassy samples of dGuo, its ^{15}N-substituted derivatives, and 8-D-dGuo were γ-irradiated with an absorbed dose of 2.5 kGy at 77 K and were also stored at 77 K.

Annealing of Samples. As in our earlier work,[8] a variable temperature assembly was employed that passed cooled dry nitrogen gas over the sample. A copper−constantan thermocouple was used to monitor temperatures. The glassy samples (7.5 M LiCl) were annealed to 150−155 K for 10−15 min, resulting in loss of (light-yellow) $Cl_2^{\bullet-}$ and the concomitant formation of one-electron oxidized dGuo radicals, as evidenced by their ESR spectra and color development in the samples: red-violet at pH ≤ 9 and blue at pH ≥ 11.[8b]

Electron Spin Resonance. ESR spectra were taken on a Varian Century series ESR spectrometer operating at 9.2 GHz with an E−4531 dual cavity, 9 in. magnet, and with a 200 mW klystron. After γ-irradiation at 77 K and annealing to 150−155 K, samples were immediately immersed in liquid nitrogen, and an ESR spectrum was recorded at 77 K and 40 dB (20 μW).[8] Fremy's salt (with $g = 2.0056$, $A_N = 13.09$ G) was used for field calibration similar to our previous works.[8] We have carried out the spectral simulations using SimFonia and WIN-EPR (Bruker). As in our previous work with glassy samples,[8] a small singlet "spike" from irradiated quartz at $g = 2.0006$ was subtracted from spectra before analysis.

Simulations of ESR Spectra. Simulations of anisotropic ESR spectra were performed with the WIN-EPR (Bruker) program. Anisotropic nitrogen couplings and g values were found by fits of simulated spectra to the 8-D-dGuo experimental spectra of $G^{\bullet+}$, $G(-H)^{\bullet}$, and $G(-2H)^{\bullet-}$ found as the pH was adjusted to 3, 9, and 12, respectively. These values were then employed in the simulations of the dGuo spectra of these three one-electron oxidized species. The major axis of the nitrogen coupling (A_{zz}) was assumed to be collinear with that of the intermediate value of the C8(H) coupling, which has near-zero anisotropic contribution. This assumes the p_z-orbitals of the π−electron system are coaxial. The radicals in the three prototropic forms were calculated by DFT to be only slightly nonplanar, thus the assumption that A_{zz} for the guanine moiety nitrogen atoms is collinear with A_{zz} for C8(H) is a good approximation. We performed dozens of computer simulations of the ESR spectra for each species and have been able to ascertain error limits of our fits of ±1 G for the largest of the nitrogen anisotropic couplings and ±1 G for each of the three components of the C8(H) anisotropic coupling (see Supporting Information Figure S1 for examples of simulations which support this.) The smallest nitrogen anisotropic couplings (A_{xx} and A_{yy}) could not be observed, as they are small and unresolved (Table 1). They were assumed to be zero in our simulations and the line width was adjusted to account for unresolved couplings. With the aid of the same line widths, the same C8(H) couplings, and the same g values, the anisotropic N hyperfine couplings in $G^{\bullet+}$, $G(-H)^{\bullet}$, and $G(-2H)^{\bullet-}$ were then further verified by employing ^{15}N (spin = $^1/_2$, gyromagentic ratio = 1.404 with respect to ^{14}N (spin = 1)) substituted derivatives of dGuo: [2-^{15}N]-dGuo, [1,2-^{15}N]-dGuo, and [1,2,3-^{15}N]-dGuo. Because ^{15}N couplings are 1.404 times those of ^{14}N and have a spin of $^1/_2$ vs a spin of

TABLE 1: Experimental and Theoretical[a] ESR Parameters for $G^{\bullet+}$, G(−H)•, and G(−2H)•−

		8-D-dGuo/dGuo[b]						dGuo			
		^{14}N3 couplings(G)			^{14}N2 couplings(G)			C8(H) Coupling (G)			8-D-dGuo/dGuo
radical		A_{zz}	A_{xx}	A_{yy}	A_{zz}	A_{xx}	A_{yy}	A_{zz}	A_{xx}	A_{yy}	*g*-values (experimental)
$G^{\bullet+}$	exp[c,d,e]	13.0	∼0	∼0	6.5	∼0	∼0	−7.5	−10.5	−3.5	$g_{xx} = 2.0045$
	theory										$g_{yy} = 2.0045$
	$G^{\bullet+} + 7\ H_2O$	11.8	0.8	0.8	9.1	0.6	0.6	−7.8	−10.4	−2.4	$g_{zz} = 2.0021$
G(−H)•	exp[c,d,e]	12.0	∼0	∼0	8.0	∼0	∼0	−7.2	−10.5	−3.5	$g_{xx} = 2.0041$
	theory										$g_{yy} = 2.0041$
	G(N1−H)• + 7 H_2O	13.5	0.8	0.9	9.1	0.6	0.7	−8.4	−11.3	−3.0	$g_{zz} = 2.0021$
	G(N2−H)• + 7 H_2O	15.0	1.0	1.0	17.6	0.8	0.8	−6.6	−8.8	−2.3	
G(−2H)•−	exp[c,d,e]	13.2	∼0	∼0	16.2	∼0	∼0	−5.5	−7.5	−2.5	$g_{xx} = 2.0042$
	theory										$g_{yy} = 2.0042$
	G(−2H)•−+9 H_2O	14.8	0.9	1.0	17.6	0.8	0.8	−6.8	−9.3	−2.6	$g_{zz} = 2.0025$
	G(−2H)•−+10 H_2O	15.1	1.0	1.0	15.5	0.7	0.7	−7.2	−9.8	−2.7	

[a] Structures optimized and hyperfine couplings calculated using DFT (B3LYP) with a 6-31G(d) basis set. [b] Experimental nitrogen hyperfine couplings and g values were measured in 8-D-dGuo and these were then employed to simulate the spectra of $G^{\bullet+}$, G(−H)•, and G(−2H)•− in dGuo. [c] Experimental A_{xx} and A_{yy} nitrogen hyperfine couplings of value ca. zero are within the line width and too small to be characterized. Theoretical values confirm the small values of these couplings. [d] Line shapes used were generally Lorenztian for the 8-D-dGuo and Gaussian for dGuo radical species. The C8(H) coupling creates a superposition of line components at various orientations best simulated with the Gaussian line shape. [e] ^{15}N (spin = $^1/_2$) couplings are 1.404 times the nitrogen couplings (^{14}N, spin = 1) shown above.

TABLE 2: Relative Stabilities of G(N1−H)• and G(N2−H)• Calculated Using Different Methods and Basis Sets

			relative stability (kcal/mol)	
method	ref	parent atructure	G(N1−H)•	G(N2−H)•[a]
B3LYP/6-31G(D)	this work	dGuo + H_2O	2.65	0.00, 3.63 anti
		(solution)[b]	(0.90)	(0.00)
B3LYP/6-31G(D)	this work	dGuo+7 H_2O	0.00	3.26
		(solution)[b]	(0.00)	(3.00)
B3LYP/6-31G*[c]	this work	9-Met-Gua H_2O	2.80	0.00
B3LYP/6-31++G(3df,3pd)//		guanine	4.71	0.00
B3LYP/6-31++G(3df,3pd)[d]	6b	(solution)	(0.00)	(0.91)
B3LYP/6-311G(2pd,p)//6-31G**	6b	guanine	4.43[e]	0.00
CPMD[f]	6b	guanine	3.73	0.00
B3LYP/DZP++[g]	6d	guanine	4.96	0.00, 4.76 anti

[a] Unless otherwise stated, G(N2−H)• refers to syn conformer, $G(N2-H)^{\bullet}_{syn}$. [b] PCM solvation model. [c] Relative stabilities calculated by us by substituting methyl (CH_3) group at the N9 site of the guanine radical in the presence of a single water molecule placed between N1 and N2 side of the 9-methyl guanine radical. [d] The solvation free energies using COSMO model are given in the parentheses. [e] Enthalpy calculated at 0K. [f] Car−Parrinello molecular dynamics (CPMD) method. [g] Zero-point vibration corrected energies.

1, a substantial change in the resultant spectrum is observed. This provides an excellent test for our analyses based on ^{14}N couplings.

DFT Calculations. Geometries of $G^{\bullet+}$, G(−H)• (singly deprotonated $G^{\bullet+}$ in dGuo) in two different tautomeric forms, and G(−2H)•− (doubly deprotonated $G^{\bullet+}$), including seven and more water molecules, were optimized using Becke's three-parameter exchange functionals (B3)[11] with Lee, Yang, and Parr's correlational functional (LYP)[12] and 6-31G(d) basis set as implemented in the Gaussian03 suite of programs.[13a] It has been noted that, to obtain reliable values of isotropic HFCCs, calculations need a well-defined basis set.[13b,c] It has been found that reliable values of anisotropic HFCCs can be obtained with the 6-31G(d) basis set employed in this work for hydrated $G^{\bullet+}$, G(−H)•, and G(−2H)•−. Frequency animation analysis and molecular modeling were done using the JMOL molecular modeling program.[14] Calculated relative stabilities and hyperfine coupling constants (HFCCs) of selected atoms are presented in Tables 2 and 3 (and also in Supporting Information), respectively. The polarized continuum model (PCM), as implemented in the Gaussian 03 suite (IEFPCM) based on the integral equation formalism (IEF) model,[13d−g] was used to consider the effect of bulk water on the relative stabilities of the two tautomers of G(−H)•.

Results and Discussion

UV−Vis Spectra. The UV−visible spectra of the one-electron oxidized dGuo, at different pHs, taken at 77 K in a 7.5 M LiCl glass, are shown in Figure 1. These spectra are similar to those reported in the literature for one-electron oxidized Guo and dGuo in aqueous solution at room temperature.[4a,b,5] The similarities of UV−vis spectra for $G^{\bullet+}$ and G(−H)• clearly suggests that these species have a similar electronic nature.

ESR Studies. From previous ESR, ENDOR, and theoretical studies[6,7] on $G^{\bullet+}$ in dGuo, we expect three major anisotropic couplings, two nitrogen couplings (at N2 and N3), and one hydrogen (at C8 in the guanine moiety). These studies show the spin density at N1 is quite small. Because we use a D_2O solution in our work, the N−H proton couplings at N1 and at N2 are not observable because they are exchangeable and deuterons have a smaller magnetic moment than protons. A deuteron shows couplings that are only 15% (1/6.514) that of protons in the same environment.[8b,9] Therefore, to simplify the spectra, we have also deuterated the C-8 position in dGuo to get 8-D-dGuo and reduce the anisotropic ca. 8 G proton hyperfine coupling to an unresolved deuteron coupling (ca. 1.2 G). This narrows the line widths and improves resolution significantly.[8b,9] As a result, we have used 8-D-dGuo at different pHs in 7.5 M LiCl glass to facilitate the analysis for the nitrogen

TABLE 3: B3LYP/6-31G(d) Calculated Hyperfine Coupling Constants (HFCCs) and Spin Densities at Different Atoms of $G^{\bullet+}$, G(N1−H)•, G(N2−H)•, and $G(-2H)^{\bullet-}$ in the Presence of Water Molecules

species	atom no.	spin densities	hyperfine couplings (Gauss)[a] A_{iso}	T_{zz}	T_{yy}	T_{xx}
$G^{\bullet+} + 7H_2O$	N1	−0.019	−0.70	0.38	0.32	−0.65
	N2	0.190	3.41	5.67	−2.79	−2.88
	N3	0.245	4.33	7.51	−3.48	−3.54
	N7	0.025	0.51	1.46	−0.70	−0.77
	C8- - -H	0.226 [b]	−6.86	−0.91	4.41	−3.50
$G(N1-H)^{\bullet} + 7H_2O$	N1	−0.018	−0.47	0.30	0.28	−0.58
	N2	0.188	3.44	5.63	−2.77	−2.87
	N3	0.281	5.08	8.44	−4.21	−4.23
	N7	−0.009	−0.06	0.56	−0.24	−0.32
	C8- - -H	0.245[b]	−7.58	−0.81	4.55	−3.74
$G(N2-H)^{\bullet} + 7H_2O$	N1	0.027	0.34	1.78	−0.85	−0.33
	N2	0.399	6.47	11.16	−5.57	−5.60
	N3	0.316	5.69	9.34	−4.63	−4.71
	N7	−0.003	0.00	0.63	−0.29	−0.34
	C8- - -H	0.189 [b]	−5.90	−0.66	3.59	−2.93
$G(-2H)^{\bullet-} + 9H_2O$	N1	0.030	0.34	0.75	−0.35	−0.40
	N2	0.397	6.4	11.24	−5.61	−5.63
	N3	0.314	5.59	9.23	−4.57	−4.66
	N7	−0.038	−0.56	0.23	0.16	−0.39
	C8- - -H	0.202[b]	−6.23	−0.56	3.63	−3.06
$G(-2H)^{\bullet-} + 10H_2O$	N1	0.016	0.07	0.34	−0.14	−0.20
	N2	0.347	5.65	9.82	−4.91	−4.91
	N3	0.320	5.71	9.41	−4.67	−4.75
	N7	−0.036	−0.52	0.22	0.12	−0.34
	C8- - -H	0.213[b]	−6.56	−0.60	3.82	−3.22

[a] $A_{ii} = \mathcal{A}_{iso} + T_{ii}$, as discussed in the text. [b] The spin density on the C atom at C-8.

hyperfine couplings and *g* values. These couplings and *g* values are then used in the analysis of the corresponding ESR spectra in identically prepared glassy samples of dGuo studied at each pH. Further, employing identically prepared glassy samples of ^{15}N-substituted derivatives of dGuo ([2-^{15}N]-dGuo, [1,2-^{15}N]-dGuo, and [1,2,3-^{15}N]-dGuo, we have verified the assignment to site as well as the magnitude of the ^{14}N couplings in $G^{\bullet+}$, $G(-H)^{\bullet}$, and $G(-2H)^{\bullet-}$.

Figure 2 shows the effect of pH on the formation of $G^{\bullet+}$ in glassy samples of 8-D-dGuo (Figure 2A−C) and of dGuo (Figure 2D−F) prepared in 7.5 M LiCl glass in D_2O. Figure 3 shows identically prepared samples of [2-^{15}N]-dGuo and of [1,2-^{15}N]-dGuo (Figure 3A−C), and of [1,2,3-^{15}N]-dGuo (Figure 3D−F).

$G^{\bullet+}$ in 8-D-dGuo, dGuo, and in ^{15}N-Substituted Derivatives of dGuo. In Figure 2A and D, we show the ESR spectra (black color) of $G^{\bullet+}$ formed in glassy samples of 8-D-dGuo and of dGuo at pH 3 in 7.5 M LiCl, after reaction with $Cl_2^{\bullet-}$ as done in our earlier work.[8] At this pH, $G^{\bullet+}$ is not deprotonated. The experimental spectra found in 8-D-dGuo was simulated using the hyperfine couplings and *g*-values given in Table 1 ("experimental values"). This simulation matches the corresponding experimental spectrum quite well (Figure 2A). Because the nitrogen couplings and radical *g*-values do not change when the deuteron at C8 is replaced by a proton, the values were then used for the simulation of the spectrum of dGuo. The C8(H) anisotropic couplings for the dGuo radical were those that resulted in a good fit to the experimental dGuo spectrum (Figure 2D, Table 1).

Simulations of the ^{15}N (spin = $^1/_2$) substituted ESR spectra for ([2-^{15}N]-dGuo), ([1,2-^{15}N]-dGuo), and ([1,2,3-^{15}N]-dGuo) (Figure 3) for $G^{\bullet+}$, $G(-H)^{\bullet}$, and $G(-2H)^{-\bullet}$ were performed using identical parameters as used for the ^{14}N simulations, taking only into account the change in coupling and spin for the ^{15}N site. Thus these simulations have not been optimized to fit and provide an excellent test of our analyses for ^{14}N couplings as well as their site assignments. In each case, the simulations closely match the experimental spectra.

In Figure 3A−C, the C8−H doublet at the center in the $G^{\bullet+}$ spectrum is even more prominent than that observed for ^{14}N counterparts. This doublet again collapses to a singlet upon deuteration at C8−H in [2-^{15}N]-dGuo (see Supporting Information Figure S2). We find that $G^{\bullet+}$ formed in [2-^{15}N]-dGuo and in [1,2-^{15}N]-dGuo show identical ESR spectra (Figure 3A), which shows that N1 does not have a significant hyperfine coupling. The match between ESR spectra of $G^{\bullet+}$ formed in [1,2-^{15}N]-dGuo and in [1,2,3-^{15}N]-dGuo (Figure 3A and D) with their corresponding simulations verify our ^{14}N -hyperfine couplings magnitudes and sites (Table 1). Further they clearly show that, in $G^{\bullet+}$, the hyperfine couplings of N3 are larger than those of N2 (Table 1).

$G(-H)^{\bullet}$ in 8-D-dGuo, dGuo, and in ^{15}N-Substituted Derivatives of dGuo. In Figure 2B and E, we present the ESR spectra (black) in glassy samples of 8-D-dGuo and of dGuo at pH ca. 9 in 7.5 M LiCl after reaction with $Cl_2^{\bullet-}$. At this pH, $G^{\bullet+}$ has undergone a single deprotonation[8b] at N1 (vide infra) to form $G(-H)^{\bullet}$. Resolved line components from anisotropic nitrogen atom couplings are visible in wings of these spectra of $G(-H)^{\bullet}$ (Figure 2B, E). As was done for $G^{\bullet+}$, nitrogen hyperfine parameters were found by analysis of the experimental spectra of 8-D-dGuo, and these values, along with an anisotropic

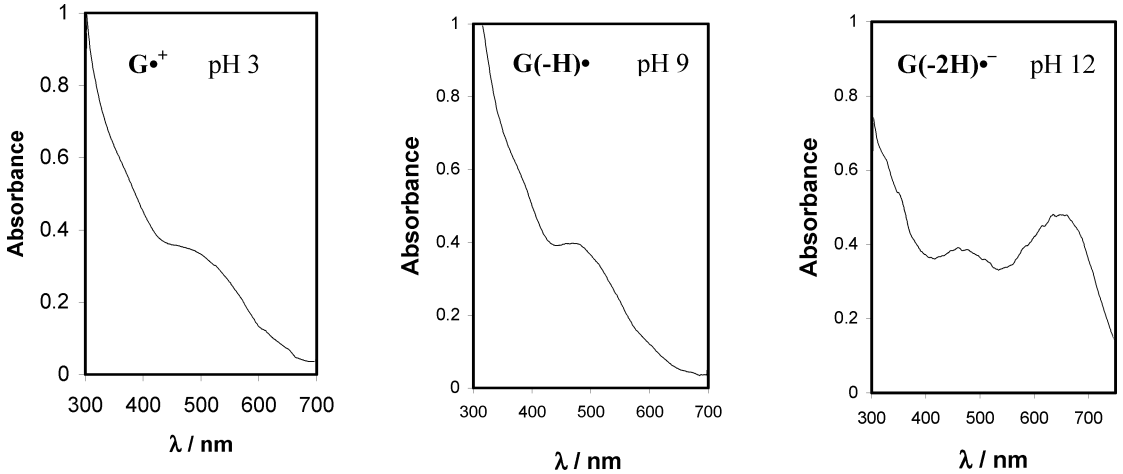

Figure 1. UV−Visible absorption spectra of one-electron oxidized guanine moiety-$G^{\bullet+}$, $G(-H)^{\bullet}$, and $G(-2H)^{\bullet-}$, respectively, produced by $Cl_2^{\bullet-}$ oxidation of dGuo at 77 K in 7.5 M LiCl glass/D_2O with pH.

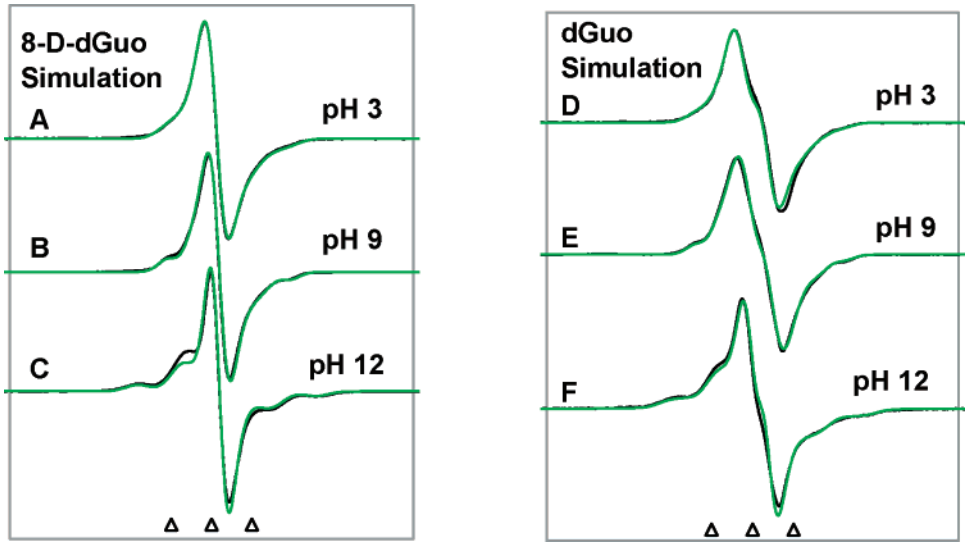

Figure 2. ESR spectra found for one-electron oxidized 8-D-dGuo (A−C) (black), dGuo (D−F) (black) at various pHs in 7.5 M LiCl glasses at 77 K. The ESR parameters, hyperfine couplings, and *g*-values, used for the simulated spectra (green) are given in Table 1. Our results indicate that $G^{\bullet+}$ is found at pHs ≤ 5, $G(N1-H)^{\bullet}$ is found at pH 7−9, and $G(-2H)^{\bullet-}$ is found at pH ca. 12. All spectra were recorded at 77 K. The three reference markers in all figures are Fremy's salt resonances with the central marker at $g = 2.0056$, and each of three markers is separated from one another by 13.09 G.

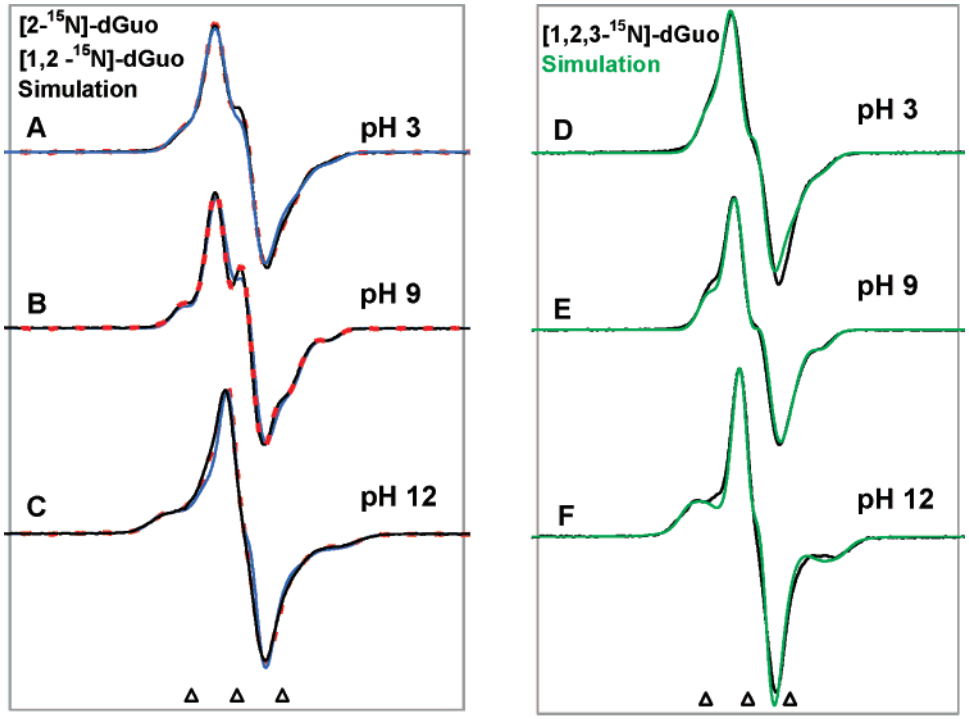

Figure 3. ESR spectra found for one-electron oxidized [2-^{15}N]-dGuo (Black) and [1,2-^{15}N]-dGuo (broken red) (A−C), [1,2,3-^{15}N]-dGuo (black) (D−F) at various pHs in 7.5 M LiCl glasses at 77 K. The ESR parameters, hyperfine couplings, and *g*-values, used for the simulated spectra, are given in Tables 1 with ^{15}N (spin = $^1/_2$) couplings at ^{15}N-substituted sites equal to 1.404 times the ^{14}N (spin = 1) couplings. The close fits of the simulated spectra in black to experiment both verify the ^{14}N coupling magnitudes as well as the sites of the couplings. In A−C, the fact that [2-^{15}N]-dGuo and [1,2-^{15}N]-dGuo give identical spectra shows that the N1 site does not have a significant coupling.

C8−H proton coupling, were used to fit the dGuo spectrum. The simulated spectra (green color) using these parameters (Table 1, $G(N1-H)^{\bullet}$) match the corresponding experimentally obtained spectra of $G(-H)^{\bullet}$ in both 8-D-dGuo and dGuo samples; it should be noted that the single deprotonation of $G^{\bullet+}$ has only a small effect on the C8(H) hyperfine couplings. We also note that both UV−vis spectra (Figure 1) and the ESR spectra (Figure 2) of $G^{\bullet+}$ and $G(-H)^{\bullet}$ are very similar for dGuo as well as 8-D-dGuo samples. The similarities in ESR spectra of $G^{\bullet+}$ and $G(-H)^{\bullet}$ are justified by the fact that the spin densities and the associated hyperfine couplings for these two species are similar (Tables 1 and 3). It is, however, evident from Table 1 and Figure 4 that the $g_{\perp}$ values of these two radicals differ enough to distinguish the state of protonation with pH.

Again, the experimentally obtained N-hyperfine couplings for $G(-H)^{\bullet}$ (Table 1) were validated by ^{15}N hyperfine parameters of $G(-H)^{\bullet}$ formed in [2-^{15}N]-dGuo, [1,2-^{15}N]-dGuo and in [1,2,3-^{15}N]-dGuo (Figure 3B and E). These spectra clearly establish that (i) in $G(-H)^{\bullet}$, the hyperfine couplings of N3 are larger than those of N2, and (ii) N1 does not have significant

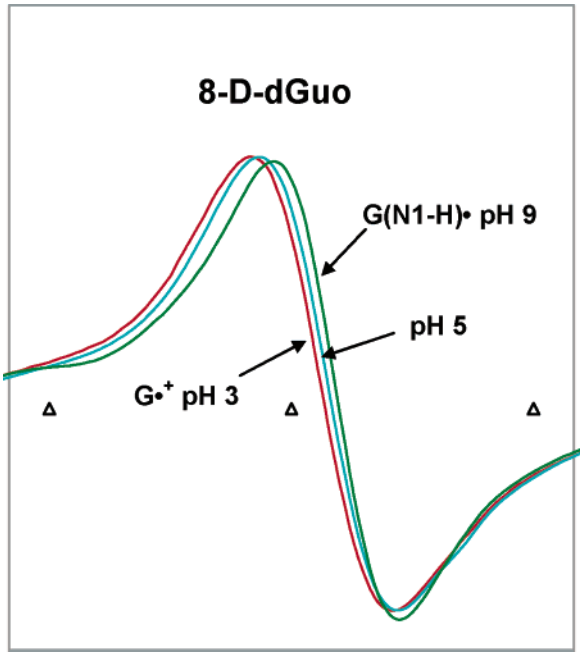

Figure 4. ESR spectra for one-electron oxidized 8-D-dGuo in a 7.5 M LiCl glass at 77 K showing the difference in the field positions of the central components (apparent $g_\perp$ values) of $G^{\bullet+}$ (pH = 3) and G(N1−H)• (pH = 9). The fact that the apparent *g*-value of the ESR spectrum at pH 5 is near the average of those obtained at pH 3 and pH 9 suggests that, at pH = 5, about equal amounts of G(N1−H)• and $G^{\bullet+}$ are present.

hyperfine coupling in the ESR spectra of G(−H)• (Table 1). As we have seen in the spectra for $G^{\bullet+}$ (Figure 2G, H), the C8−H doublet at the center also becomes prominent due to ^{15}N isotopic substitution in the spectra of G(−H)• (Figure 3B, E and the Supporting Information Figure S2).

G(−2H)$^{\bullet-}$ in 8-D-dGuo, dGuo, and in ^{15}N-Substituted Derivatives of dGuo. From previous work,[4a,b,5] it appears that at pH = 12, $G^{\bullet+}$ is doubly deprotonated (at N1 and N2), resulting in $G(-2H)^{\bullet-}$. In Figure 2C and F, the ESR spectra (black color) of $G(-2H)^{\bullet-}$ formed in glassy samples of 8-D-dGuo and of dGuo at pH ca. 12 in 7.5 M LiCl, after reaction with $Cl_2^{\bullet-}$, are shown. Nitrogen hyperfine couplings are nicely resolved in the wings of both spectra. Figure 2C for 8-D-dGuo and Figure 2F for dGuo clearly demonstrate excellent resolution in the wings of the anisotropic N-couplings for $G(-2H)^{\bullet-}$ for both C8-deuterated and protonated systems. The poorly resolved ca. 5.5 G doublet from C8(H) is lost in 8-D-dGuo as expected. Again, the simulated spectra (green) using the parameters in Table 1 match the experimental spectra well.

ESR spectra of $G(-2H)^{\bullet-}$ in [2-^{15}N]-dGuo, [1,2-^{15}N]-dGuo, and [1,2,3-^{15}N]-dGuo are shown in Figure 3C and F. Analyses of spectra shown in Figure 3C and F clearly establish that (i) in the ESR spectrum of $G(-2H)^{\bullet-}$, N1 does not have a significant hyperfine coupling (Table 1), and (ii) unlike the cases of $G^{\bullet+}$ and G(−H)•, N2 has a larger nitrogen hyperfine coupling than N3. Figure S2 in Supporting Information shows the collapse of the C8−H doublet on deuteration in [2-^{15}N]-dGuo at various pHs.

From the analyses of the ESR spectra of one-electron oxidized guanine in 8-D-dGuo and ^{15}N-substituted derivatives of dGuo ([2-^{15}N]-dGuo, [1,2-^{15}N]-dGuo, and [1,2,3-^{15}N]-dGuo**)** at different pHs, we are confident that the anisotropic N-couplings are well determined (±1 G) (see Supporting Information Figure S3). We note that the increase of the total width in the spectrum on going from 8-D-dGuo to dGuo in each pH range gives the A_{zz}(C8−H) coupling (after properly accounting for the small deuterium coupling). Because the nitrogen couplings are well determined, the C8(H) couplings are likely to also be accurate to within ±1 G. Numerous fits that varied the couplings suggest these uncertainties are reasonable (see Supporting Information Figures S1 and S3). The values of the hyperfine coupling constants for the N2, N3, and C8(H) are in good agreement with the both existing ESR and ENDOR studies[7,8] and with our theoretical calculations (vide infra).

The ESR measurements at the various pHs used indicate that the pK_a of $G^{\bullet+}$ in our system (aqueous D_2O glasses at 77 K) is between 5 and 6; this is approximately 1 to 2 pH units higher than the corresponding pK_a (ca. 3.9) of $G^{\bullet+}$ in aqueous H_2O solution at 298 K.[1,4−7] This is reasonable, considering the system is a D_2O solution (glassy) at low temperature and that pK_as in D_2O are generally higher than the corresponding pK_a's in H_2O (Figure 4).[15] These results are also in accord with our previous work on photoexcitation of $G^{\bullet+}$ in D_2O glass at 77 K, which suggested that $G^{\bullet+}$ does not deprotonate until ca. pH 6.[8]

DFT Calculations

Relative Stabilities of Different Tautomeric Forms. The presence of different tautomeric forms of G(−H)• in DNA are of considerable interest and of biological significance.[7] ESR measurements give hyperfine couplings that are sensitive to these tautomeric forms and afford an opportunity to find the dominant tautomer in a vacuum and an aqueous environment by using a combination of theory and experiment. In this DFT study, we consider three possible tautomers of G(−H)•: (i) deprotonation at N1 to give G(N1−H)• and (ii) deprotonation at either the syn or anti sites of the NH_2 group with respect to the N3 atom (Scheme 1). The geometries of all three tautomers in the presence of a single water molecule, placed near the N1 and NH_2 sites of the molecule, were fully optimized using the B3LYP/6-31G(d) level of theory. The relative stabilities of the three structures G(N1−H)• + H_2O, $G(N2-H)^{\bullet}_{syn}$ + H_2O, and $G(N2-H)^{\bullet}_{anti}$ + H_2O were 2.65, 0.00, and 3.63 kcal/mol, respectively (Table 2). Recently, Schaefer and co-workers, using the B3LYP/DZP++ level of theory, found that G(N2−H)• was more stable than G(N1−H)• by 4.96 kcal/mol.[6d] To take into account the effect of the solvent better, we performed a single-point calculation of the optimized tautomers G(N1−H)• + H_2O and G(N2−H)• + H_2O in an aqueous environment (ϵ_0 = 78.4) using the polarized continuum model (IEFPCM) at the B3LYP/6-31G(d) level of theory. Using IEFPCM to model the aqueous environment, G(N2−H)• + H_2O is only 0.90 kcal/mol more stable than G(N1−H)• + H_2O (Table 2).

Regarding the relative stabilities of G(N1−H)• and $G(N2-H)^{\bullet}_{syn}$, values in guanine calculated at various theoretical levels are also shown in Table 2. Using different methods and basis sets, Mundy et al.[6b] calculated the relative stabilities of several radicals that were generated from the deprotonation of $G^{\bullet+}$ at different sites. Their calculations (B3LYP/6-31++G(3df,3pd)//B3LYP/6-31++G(3df,3pd)) showed that $G(N2-H)^{\bullet}_{syn}$ was more stable than G(N1−H)• in the gas phase by 4.71 kcal/mol (see Table 2). However, using the same basis set and the COSMO solvation model to simulate an aqueous environment, they found that G(N1−H)• was more stable than G(N2−H)• by 0.91 kcal/mol. The same trend is found in all reported calculations, which agree that $G(N2-H)^{\bullet}_{syn}$ state is more stable than G(N1−H)• in the gas phase by 2.7 to 5.0 kcal/mol.[7]

On the basis of these studies, we have further included the water molecules surrounding the guanine base to test the effects of hydration on the relative stabilities of G(N1−H)• and G(N2−

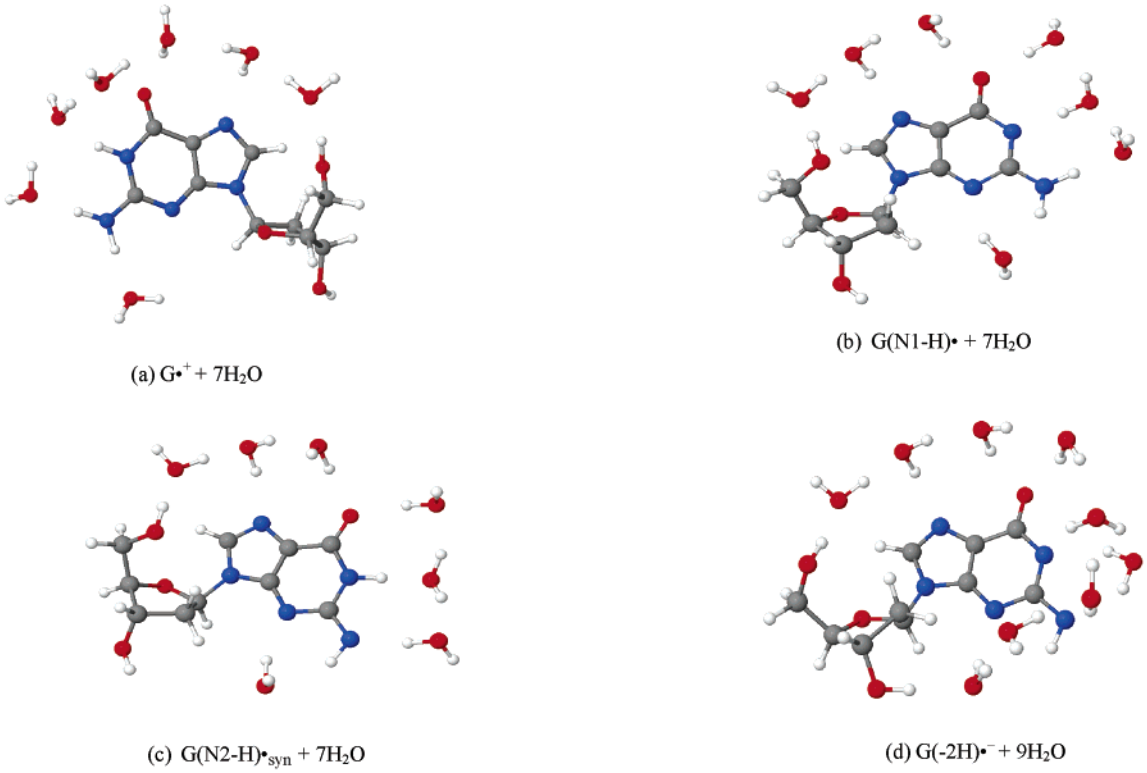

Figure 5. Optimized structures of (a) $G^{\bullet+}$, (b) $G(N1-H)^{\bullet}$, (c) $G(N2-H)^{\bullet}_{syn}$, and (d) $G(-2H)^{\bullet-}$ in the presence of water molecules. The geometries were fully optimized using B3LYP/6-31G(d) method.

$H)^{\bullet}_{syn}$ (Figure 5). We have fully optimized each structure using B3LYP/6-31G(d) level of calculation, including seven water molecules around the guanine base moiety.

These calculations indicate that $G(N1-H)^{\bullet} + 7H_2O$ is more stable than $G(N2-H)^{\bullet}_{syn} + 7H_2O$ by 3.26 kcal/mol (see Table 2). To take into account the effect of full solvent, we have further performed single-point calculations using the optimized geometries of $G(N1-H)^{\bullet} + 7H_2O$ and $G(N2-H)^{\bullet}_{syn} + 7H_2O$, along with the IEFPCM model at the B3LYP/6-31G(d) level. These calculations show that $G(N1-H)^{\bullet} + 7H_2O$ is still more stable than $G(N2-H)^{\bullet} + 7H_2O$ by 3.00 kcal/mol (Table 2). Thus our results suggest that hydration is most important on the relative stabilities of these two tautomers.

Hydrogen Bond Energies. The hydrogen bonding energy arising from seven waters is calculated using the following eq 1:

$$E^{H-bond} = TE^{G(-H)\bullet+7H_2O} - (TE^{G(-H)\bullet} + 7TE^{H_2O}) \quad (1)$$

Here E^{H-bond} is the hydrogen bond energy, *TE* is the total energy of the optimized $(G(-H)^{\bullet} + 7H_2O)$ complex, and $TE^{G(-H)\bullet}$ refers to the total energy of either $G(N1-H)^{\bullet}$ or $G(N2-H)^{\bullet}_{syn}$ tautomer. TE^{H_2O} is the total energy of a single H_2O molecule.

Using eq 1, $E^{H-bond}[G(N1-H)^{\bullet}] = -104.1$ kcal/mol and $E^{H-bond}[G(N2-H)^{\bullet}_{syn}] = -95.6$ kcal/mol (Figure 5). Thus, the hydrogen bonding due to hydration stabilizes $G(N1-H)^{\bullet}$ by 8.5 kcal/mol more than it does $G(N2-H)^{\bullet}$. Note from Figure 5 that the same number of hydrogen bonds (twelve) are present in each system and it is the increased *strength* of the hydrogen bonds in the $G(N1-H)^{\bullet} + 7H_2O$ system that accounts for the additional stabilization energy.

Hyperfine Coupling Constants in $G^{\bullet+}$ and $G(-H)^{\bullet}$. On comparing experimental HFCCs with those calculated at various hydration levels (see Supporting Information), we find those calculations using seven water molecules for $G^{\bullet+}$, $G(N1-H)^{\bullet}$, and $G(N2-H)^{\bullet}_{syn}$ (Figure 5) and 8−10 water molecules for $G(-2H)^{\bullet-}$ (Figure 5) in dGuo gave the best fit to experiment (see Table 1 and Table 3).

For $G^{\bullet+} + 7H_2O$, B3LYP/6-31G(d) level of theory predicts two observable A_{zz} nitrogen couplings of 11.8 G for N3 and 9.1 G for N2 and a substantial anisotropic hydrogen coupling for C8(H) of (−7.8, −10.4, −2.4) G. These values are all in good agreement with our experimental couplings (Table 1). The calculated hyperfine coupling constants for N1 and N7 (Tables 1 and 3) are small, and these couplings were not observed in our ESR experiments for $G^{\bullet+}$.

For $G(N1-H)^{\bullet} + 7H_2O$, the calculated A_{zz} values for N3 (13.5 G) and N2 (9.1 G), and the calculated anisotropic C8(H) coupling (−8.4, −11.3, −3.0) G, agree well with the corresponding experimental values of 12.0 G, 8.0 G, and (−7.2, −10.5, −3.5) G (Table 1). Calculations also indicate that N1 and N7 both have very small couplings (Table 3), in strong agreement with the fact that these couplings were not observed in our ESR experiments. In addition, our calculated anisotropic HFCC for C8(H) is in good agreement with that calculated by Wetmore et al.,[6a] (−7.0, −11.5, −3.9) G using DFT (P86) with a 6-311G(2d,p) basis set. On the other hand, for $G(N2-H)^{\bullet}_{syn} + 7H_2O$, the calculated A_{zz} HFCCs for N2 (17.6 G) and N3 (15.0 G) and the calculated anisotropic C8(H) coupling (−6.6, −8.8, −2.3) G, do not agree well with the corresponding experimental values. The large calculated A_{zz} for N2 (17.60 G) calculated for $G(N2-H)^{\bullet}$ is not in agreement with the smaller experimental value of 8.0 G. Experiment is in far better agreement with the 9.1 G for the N2 A_{zz} coupling predicted for $G(N1-H)^{\bullet}$. The C8(H) anisotropic couplings calculated by Wetmore et al.[6a] for $G(N2-H)^{\bullet}$ of (−6.3, −9.4, −2.3) G are in close agreement with our calculated values. For $G(N2-H)^{\bullet}$ also, calculations indicate that N1 and N7 have very small couplings (Table 3).

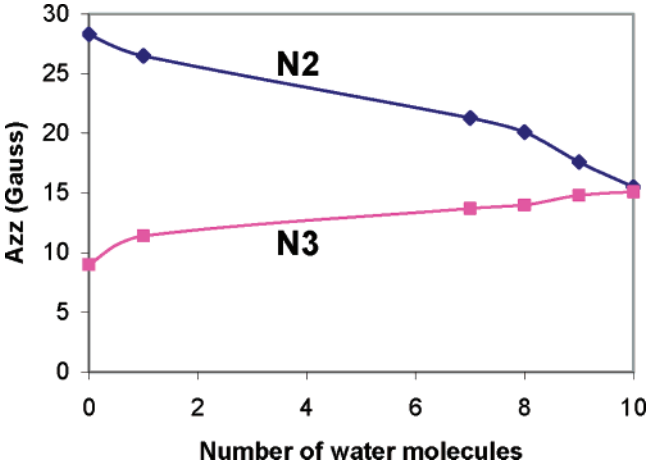

Figure 6. Variation of hyperfine coupling constant A_{zz} (Gauss) at N2 and at N3 sites of G(−2H)$^{\bullet-}$ with number of water molecules of hydration. Calculations were done using B3LYP/6-31G(d) method.

These results strongly suggests that G(N1−H)$^{\bullet}$ is the most stable tautomer present in an aqueous medium, and therefore, by combining the ESR and DFT results, we conclude N1 is the site of deprotonation for G$^{\bullet+}$ in this frozen aqueous glass.

Hyperfine Coupling Constants in G(−2H)$^{\bullet-}$. The calculated A_{zz} for N2 in G(−2H)$^{\bullet-}$ depends quite strongly on the number of water molecules included in the model (Figure 6). We found that only on increasing the number of hydration waters to the 9−10 range could we obtain nitrogen A_{zz} couplings that compared favorably with experiment. For G(−2H)$^{\bullet-}$ + 9H_2O, the predicted HFCCs at N3 (14.8, 0.9, 1.0) G and N2 (17.6, 0.8, 0.8) G and the anisotropic C8(H) coupling (−6.8, −9.3, −2.6) G are in reasonable agreement with the observed couplings (Table 1).

From Figure 6, it is evident that in G(−2H)$^{\bullet-}$, the HFCC (A_{zz}) at the N2 atom decreases with increasing number of hydrating water molecules while that of N3 increases. With 10 water molecules, these values become nearly equal. We find that the Mulliken spin densities at N2 and N3 atoms are also nearly equal, 0.35 and 0.32. Because G(−2H)$^{\bullet-}$ is negatively charged and is in solution of 7.5 M LiCl (Figure 2), we also performed calculations including Li^+ as a counterion. We find that, in the presence 7−10 water molecules, Li^+ has a very small effect on HFCCs, suggesting water hydrogen bonding dominates over the electrostatic effects. However, in the presence of a small number of water molecules, the Li^+ effect is substantial, with the same effect as for increased hydration (see Supporting Information). Analyses of the ESR spectra (spectra C, F, Figure 3) for ^{15}N (spin = $^1/_2$) HFCCs clearly show that, for G(−2H)$^{\bullet-}$, the N2 site has a slightly larger coupling than N3, in agreement with results shown in Figure 6 at about nine water molecules of hydration.

ESR studies employing 8-D-dGuo at different pH and the complementary theoretical calculations for G(−2H)$^{\bullet-}$ suggest that N7 has only a small isotropic hyperfine coupling (ca. 0.5 G) (Table 3). An earlier computational and ESR study on G$^{\bullet+}$ in aqueous solution suggested a 3 G isotropic coupling at N7,[7k] which is significantly larger than we would expect from our work.

Activation Energy of Proton Transfer. To estimate the energetics of water-assisted proton transfer between tautomers G(N1−H)$^{\bullet}$ and G(N2−H)$^{\bullet}$, we have calculated the forward barrier for the proton transfer between G(N1−H)$^{\bullet}$ + H_2O and G(N2−H)$^{\bullet}$ + H_2O in the presence of a single water molecule (Figure 7). The B3LYP/6-31G(d) level of theory predicts a forward barrier of 18.7 kcal/mol (Figure 7). A frequency calculation shows that the transition state has a single negative frequency −1688 cm^{-1}, confirming this is a true transition state that connects the reactant and product. In another recent calculation[6f] using the B3LYP/6-31G* method, and a model in which the sugar moiety was replaced by a methyl group (9-methylguanine), a forward barrier of 18.8 kJ/mol (4.5 kcal/mol) was reported. In our calculation, we considered the full sugar moiety (Figure 7). We therefore repeated their calculation on the 9-methylguanine system and obtained 18.9 kcal/mol for the barrier height (Table 2), suggesting the units may have been incorrectly reported in the previous work. Without any water, the direct proton transfer from N2 to N1 converting G(N1−H)$^{\bullet}$ to G(N2−H)$^{\bullet}$ has been reported to have a much larger barrier of 43.9 kcal/mol.[6f] We note the role of water molecules in

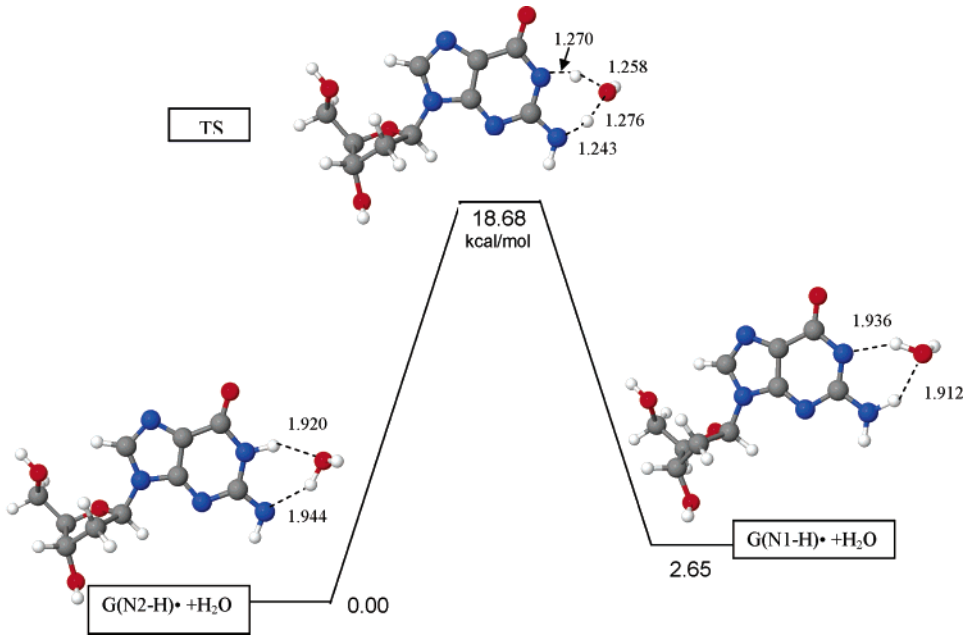

Figure 7. Water-assisted proton-transfer reaction path between G(N2−H)$^{\bullet}_{syn}$ + H_2O and G(N1−H)$^{\bullet}$ + H_2O through the transition state. The geometries were optimized and energies calculated using the B3LYP/6-31G(d) level of calculation. Bond distances in Å and energies in kcal/mol.

promoting proton-transfer reactions at much lower activation barriers is expected and has been reported in the literature for HF and MP2 level calculations.[16] On the basis of the above argument, the presence of a full aqueous medium (where the N1−H tautomer is favored) is expected to reduce the activation barrier significantly (Table 2). The calculation to locate the transition state in the presence of a full hydration shell awaits future efforts, as this will require substantial computational time.

Summary and Conclusions

(i) Protropic Forms and Site of Deprotonation in $G^{\bullet+}$. Our results identify three prototropic forms of one-electron oxidized guanine, $G^{\bullet+}$, $G(-H)^{\bullet}$, and $G(-2H)^{\bullet-}$, via ESR and UV−vis spectroscopy, which are found in the pH ranges 3−5, 7−9, and >11, respectively.

The experimentally obtained HFCCs for $G^{\bullet+}$ as well as $G(N1-H)^{\bullet}$ in dGuo match the theoretical values well. Thus, ESR spectroscopy, UV−visible spectroscopy, and complimentary theoretical calculations give strong evidence that the N1−H site is the first deprotonation site of $G^{\bullet+}$ in frozen aqueous (D_2O) glassy solutions.

(ii) Relative Stabilities of $G(N1-H)^{\bullet}$ and $G(N2-H)^{\bullet}$ and the Role of Hydration. Earlier theoretical calculations indicate that $G(N2-H)^{\bullet}$ is more stable than $G(N1-H)^{\bullet}$ in the gas phase by ca. 4.5 kcal/mol. Our work shows that, with one additional water molecule, this is reduced to 2.65 kcal/mol. However, with seven waters, the order of stabilization is reversed and $G(N1-H)^{\bullet}$ becomes more stable than $G(N2-H)^{\bullet}$ by ca. 3.3 kcal/mol (Table 2) as a result of the stabilizing effect of H-bonding interactions in the first hydration shell. Surprisingly, employing the IEFPCM solvation model in addition to the seven waters has little effect on the relative energies of the two tautomers. This finding suggests that the first seven waters are most important in determining the relative stability of the two tautomers. While no experimental value for the difference in energy between the two tautomers is available, our ESR and UV-vis experiments strongly suggest that $G(N1-H)^{\bullet}$ dominates in the aqueous phase, in agreement with theory.

(iii) Transition State for Water-Assisted Proton Transfer between $G(N2-H)^{\bullet}$ and $G(N1-H)^{\bullet}$. Using one water molecule, we find a clear transition state for water-assisted proton transfer between $G(N2-H)^{\bullet}$ and $G(N1-H)^{\bullet}$. Our DFT calculations suggest the activation barrier for this transfer is 18.7 kcal/mol. However, under full solvation, this value is likely to be significantly lower.

(iv) ($G(-2H)^{\bullet-}$). The ESR spectrum of $G(-2H)^{\bullet-}$ was first reported in our earlier work[8b] and, in this work, has been interpreted for the first time. ESR spectra display excellent resolution of two anisotropic N splittings for all the dGuo samples at pH 12 (Figure 2). For $G(-2H)^{\bullet-}$, theoretical calculations suggest a strong dependence of the spin density distribution and hyperfine couplings with the level of hydration. Very poor agreement of experimental couplings with theory occurs for isolated molecules, but agreement is much improved as nine or 10 water molecules are added.

(v) ^{15}N-Substituted Derivatives of dGuo. The use of ^{15}N-substituted derivatives of dGuo verified both the magnitude and site assignment of the nitrogen hyperfine couplings reported for N3, N2 in one-electron oxidized radicals of dGuo in three states of protonation. These results have also shown that: (a) N3 has the largest coupling of the one-electron oxidized guanine radicals, $G^{\bullet+}$ and $G(-H)^{\bullet}$. (b) For $G(-2H)^{-\bullet}$, N2 is the largest coupling site. (c) N1 has no significant coupling in $G^{\bullet+}$, $G(-H)^{\bullet}$, or $G(-2H)^{\bullet-}$.

Acknowledgment. This work was supported by the NIH NCI under grant no. R01CA045424. The authors are very grateful to Prof. Roger Jones for his very kind donation of the ^{15}N isotopically substituted dGuo derivatives employed in this study. A.A. is grateful to the authorities of the Rajdhani College and the University of Delhi for leave to work on this research program. A.K. and M.D.S. are thankful to the Arctic Region Supercomputing Center (ARSC) for a generous grant of CPU time and facilities. A.K. is personally thankful to the ARSC staff for their constant cooperation and timely help. We thank D. Khanduri and S. Collins for their aid with the experiments.

Supporting Information Available: Supporting Information is available and includes: expected error limits of our simulations, ESR spectra found for one-electron oxidized 8-D[2-^{15}N]-dGuo, dGuo, and [2-^{15}N]-dGuo at various pHs, ESR spectra for one-electron oxidized [2-^{15}N]-dGuo at various pHs along with several simulations based on different assignments of couplings to sites, theoretical hyperfine couplings for all radicals investigated, optimized geometries of each of the radical species treated in this work. This material is available free of charge via the Internet at http://pubs.acs.org.

Note added in proof. Recently a related work to the work presented here entitled "Tautomerism in the Guanyl Radical" by C. Chatgilialoglu et al., *J. Am. Chem. Soc. 128*, appeared on the web on 28th September, 2006. With the aid of pulse radiolysis as well as a theoretical model involving a single water molecule, these authors suggest that $G^{\bullet+}$ first decays to $G(N2-H)^{\bullet}$ which undergoes water assisted tautomerization to $G(N1-H)^{\bullet}$. In our present study, we have identified through experiment the formation of $G(N1-H)^{\bullet}$ as the only deprotonation species of $G^{\bullet+}$ found at low temperatures in an aqueous environment and have shown by more sophisticated theoretical models that this is the expected lowest energy path.

References and Notes

(1) For recent ESR reviews (charge transfer in DNA and in model compounds), see: (a) Becker, D.; Sevilla, M. D. In Royal Society of Chemistry Specialists Periodical Report; Gilbert, B. C., Davies, M. J., Murphy, D. M. Eds.; *Electron Spin Reson.* **1998**, *16*, 79−114. (b) Sevilla, M. D.; Becker, D. In Royal Society of Chemistry Specialist Periodical Report; Gilbert, B. C., Davies, M. J., Murphy, D. M. Eds.; *Electron Spin Reson.* **2004**, *19*, 243−278. (c) Cai, Z.; Sevilla, M. D. In Long Range Charge Transfer in DNA II; Schuster, G. B. Ed.; *Top. Curr. Chem.* **2004**, *237*, p 103. (d) Bernhard, W. A.; Close, D. M. In *Charged Particle and Photon Interactions with Matter: Chemical, Physicochemical and Biological Consequences with Applications*; Mozumdar, A., Hatano, Y. Eds.; Marcel Dekkar, Inc., New York, Basel, 2004; p 431. (e) Wagenknecht, H.-A. In *Charge Transfer in DNA: From Mechanism to Application*; Wagenknecht, H.-A. Ed.; Wiley-VCH: Weinheim, 2005; p 4. (f) von Sonntag, C. *Free-Radical-Induced DNA Damage and Its Repair*; Springer-Verlag: Berlin, Heidelberg, 2006; p 213.

(2) (a) Sevilla, M. D.; Becker, D.; Yan, M.; Summerfield, S. R. *J. Phys. Chem.* **1991**, *95*, 3409−3415. (b) Yan, M.; Becker, D.; Summerfield, S. R.; Renke, P.; Sevilla, M. D. *J. Phys. Chem.* **1992**, *96*, 1983−1989. (c) Wang, W.; Sevilla, M. D. *Radiat. Res.* **1994**, 9−17. (d) Spaletta, R. A.; Bernhard, W. A. *Radiat. Res.* **1993**, 143−150. (e) Mrozcka, N. E.; Bernhard, W. A. *Radiat. Res.* **1993**, *135*, 155−159. (f) Mrozcka, N. E.; Bernhard, W. A. *Radiat. Res.* **1995**, *144*, 251−257. (g) Cullis, P. M.; Davis, A. S.; Malone, M. E.; Podmore, I. D.; Symons, M. C. R. *J. Chem. Soc., Perkin Trans. 2* **1992**, 1409−1412. (h) Hüttermann, J.; Lange, M.; Ohlmann, J. *Radiat. Res.* **1992**, *131*, 18−23. (i) Hüttermann, J.; Röhrig, M.; Köhnlein, W. *Int. J. Radiat. Biol.* **1992**, *61*, 299−313.

(3) (a) Sovzil, D.; Jungwirth, P.; Havlas, Z. *Collect. Czech. Chem. Commun.* **2004**, *69*, 1395−1428. (b) Kumar, A.; Knapp-Mohammady, M.; Mishra, P. C.; Suhai, S. *J. Comput. Chem.* **2004**, *25*, 1047−1059. (c) Li, X.; Cai, Z.; Sevilla, M. D. *J. Phys. Chem. B* **2001**, *105*, 10115−10123. (d) Li, X.; Cai, Z.; Sevilla, M. D. *J. Phys. Chem. A* **2002**, *106*, 1596−1603. (e) Li, X.; Cai, Z.; Sevilla, M. D. *J. Phys. Chem A* **2002**, *106*, 9345−9351. (f) Rienstra-Kiracofe, J. C.; Tschumper, G. S.; Schaefer, H. F., III; Nandi, S.; Ellison, G. B. *Chem. Rev.* **2002**, *102*, 231−282. (g) Reynisson, J.; Steenken, S. *Phys. Chem. Chem. Phys.* **2002**, *4*, 527−532. (h) Close, D.

M. *J. Phys. Chem. A* **2004**, *108*, 10376−10379. (i) Crespo-Hernández, C. E.; Arce, R.; Ishikawa, Y.; Gorb, L.; Leszczynski, J.; Close, D. M. *J. Phys. Chem. A* **2004**, *108*, 6373−6377. (j) Close, D. M.; Crespo-Hernández, C. E.; Gorb, L.; Leszczynski, J. *J. Phys. Chem. A* **2005**, *109*, 9279−9283. (k) Caruso, T.; Carutenuto, M.; Vasca, E.; Peluso, A. *J. Am. Chem. Soc.* **2005**, *127*, 15040−15041. (l) Wetmore, S. D.; Boyd, R. J.; Eriksson, L. A. *Chem. Phys. Lett.* **2000**, *322*, 129−135.

(4) (a) Jovanovic, S. V.; Simic, M. G. *J. Phys. Chem.* **1986**, *90*, 974−978. (b) Jovanovic, S. V.; Simic, M. G. *Biochim. Biophys. Acta* **1989**, *1008*, 39−44. (c) Seidel, C. A. M.; Schulz, A.; Sauer, M. H. M. *J. Phys. Chem.* **1996**, *100*, 5541−5533. (d) Steenken, S.; Jovanovic, S. V. *J. Am. Chem. Soc.* **1997**, *119*, 617−618. (e) Baik, M.-H.; Silverman, J. S.; Yang, I. V.; Ropp, P. A.; Szalai, V. S.; Thorp, H. H. *J. Phys. Chem. B* **2001**, *105*, 6437−6444. (f) Langmaier, J.; Samec, Z.; Samcova, E.; Hobza, P.; Reha, D. *J. Phys. Chem. B* **2004**, *108*, 15896−15899. (g) Llano, J.; Eriksson, L. A. *Phys. Chem. Chem. Phys.* **2004**, *6*, 2426−2433. (h) Fukuzumi, S.; Miyao, H.; Ohkubo, K.; Suenobu, T. *J.* Phys. *Chem. A* **2005**, *109*, 3285−3294. (i) Cauet, E.; Dehareng, D.; Lievin, J. *J. Phys. Chem. A* **2006**, *110*, 00.

(5) (a) Candeias, L. P.; Steenken, S. *J. Am. Chem. Soc.* **1989**, *111*, 1094−1099. (b) Steenken, S. *Chem. Rev.* **1989**, *89*, 503−520. (c) Steenken, S. *Free Radical Res. Commun.* **1992**, *16*, 349−379. (d) Steenken, S.; Jovanovic, S. V.; Candeias, L. P.; Reynisson, J. *Chem.—Eur. J.* **2001**, *7*, 2829−2833. (e) Kobayashi, K.; Tagawa, S. *J. Am. Chem. Soc.* **2003**, *125*, 10213−10218.

(6) (a) Wetmore, S. D.; Boyd, R. J.; Eriksson, L. A. *J. Phys. Chem. B* **1998**, *102*, 9332−9343. (b) Mundy, C. J.; Colvin, M. E.; Quong, A. A. *J. Phys. Chem. A* **2002**, *106*, 10063−10071. (c) Gervasio, F. L.; Laio, A.; Iannuzzi, M.; Parrinello, M. *Chem.—Eur. J.* **2004**, *10*, 4846−4852. (d) Luo, Q.; Li, Q. S.; Xie, Y.; Schaefer, H. F., III. *Collect. Czech. Chem. Commun.* **2005**, *70*, 826−836. (e) von Sonntag, C. *Free-Radical-Induced DNA Damage and Its Repair*; Springer-Verlag: Berlin, Heidelberg, 2006; 220−221. (f) Chatgilialoglu, C.; Caminal, C.; Guerra, M.; Mulazzani, Q. G. *Angew. Chem., Int. Ed.* **2005**, *44*, 6030−6032.

(7) (a) Close, D. M.; Sagstuen, E.; Nelson, W. H. *J. Chem. Phys.* **1985**, *82*, 4386−4388. (b) Hole, E.; Nelson, W. H.; Close, D. M.; Sagstuen, E. *J. Chem. Phys.* **1987**, *88*, 5218−5219. (c) Close, D. M.; Nelson, W. H.; Sagstuen, E. *Radiat. Res.* **1987**, *112*, 283−301. (d) Hole, E. O.; Sagstuen, E. *Radiat. Res.* **1987**, *109*, 190−205. (e) Ravkin, B.; Herak, J. N.; Voit, K.; Hüttermann, J. *Radiat. Environ. Biophys.* **1987**, *26*, 1−12. (f) Nelson, W. H.; Hole, E. O.; Sagstuen, E.; Close, D. M. *Int. J. Radiat. Biol.* **1988**, *54*, 963−986. (g) Hole, E. O.; Sagstuen, E.; Nelson, W. H.; Close, D. M. *Free Radical Res. Commun.* **1989**, *6*, 87−90. (h) Kim, H.; Budzinski, E. E.; Box, H. C. *J. Chem. Phys.* **1989**, *90*, 1448−1451. (i) Hole, E. O.; Sagstuen, E.; Nelson, W. H.; Close, D. M. *Radiat. Res.* **1991**, *125*, 119−128. (j) Hole, E. O.; Sagstuen, E.; Nelson, W. H.; Close, D. M. *Radiat. Res.* **1992**, *129*, 1−10. (k) Bachler, V.; Hildenbrand, K. *Radiat. Phys. Chem.* **1992**, *40*, 59−68. (l) Hole, E. O.; Sagstuen, E.; Nelson, W. H.; Close, D. M. *Radiat. Res.* **1992**, *129*, 119−138.

(8) (a) Shukla, L. I.; Pazdro, R.; Huang, J.; DeVreugd, C.; Becker, D,; Sevilla, M. D. *Radiat. Res.* **2004**, *161*, 582−590. (b) Adhikary, A.; Malkhasian, A. Y. S.; Collins, S.; Koppen, J.; Becker, D.; Sevilla, M. D. *Nucleic Acids Res.* **2005**, *33*, 5553−5564. (c) Adhikary, A.; Kumar, A.; Sevilla, M. D. *Radiat. Res.* **2006**, *165*, 479−484.

(9) Hiraoka, W.; Kuwabara, M.; Sato, F. *Int. J. Radiat. Biol.* **1989**, *55*, 51−58 and references therein.

(10) Huang, X.; Yu, P.; LeProust, E.; Gao, X. *Nucleic Acids Res.* **1997**, *25*, 4758−4763.

(11) (a) Becke, A. D. *J. Chem. Phys.* **1993**, *98*, 1372. (b) Stephens, P. J.; Devlin, F. J.; Frisch, M. J.; Chabalowski, C. F. *J. Phys. Chem.* **1994**, *98*, 11623.

(12) Lee, C.; Yang, W.; Parr, R. G. *Phys. Rev. B* **1988**, *37*, 785.

(13) (a) Frisch, M. J.; Trucks, G. W.; Schlegel, H. B.; Scuseria, G. E.; Robb, M. A.; Cheeseman, J. R.; Montgomery, J. A., Jr.; Vreven, T.; Kudin, K. N.; Burant, J. C.; Millam, J. M.; Iyengar, S. S.; Tomasi, J.; Barone, V.; Mennucci, B.; Cossi, M.; Scalmani, G.; Rega, N.; Petersson, G. A.; Nakatsuji, H.; Hada, M.; Ehara, M.; Toyota, K.; Fukuda, R.; Hasegawa, J.; Ishida, M.; Nakajima, T.; Honda, Y.; Kitao, O.; Nakai, H.; Klene, M.; Li, X.; Knox, J. E.; Hratchian, H. P.; Cross, J. B.; Bakken, V.; Adamo, C.; Jaramillo, J.; Gomperts, R.; Stratmann, R. E.; Yazyev, O.; Austin, A. J.; Cammi, R.; Pomelli, C.; Ochterski, J. W.; Ayala, P. Y.; Morokuma, K.; Voth, G. A.; Salvador, P.; Dannenberg, J. J.; Zakrzewski, V. G.; Dapprich, S.; Daniels, A. D.; Strain, M. C.; Farkas, O.; Malick, D. K.; Rabuck, A. D.; Raghavachari, K.; Foresman, J. B.; Ortiz, J. V.; Cui, Q.; Baboul, A. G.; Clifford, S.; Cioslowski, J.; Stefanov, B. B.; Liu, G.; Liashenko, A.; Piskorz, P.; Komaromi, I.; Martin, R. L.; Fox, D. J.; Keith, T.; Al-Laham, M. A.; Peng, C. Y.; Nanayakkara, A.; Challacombe, M.; Gill, P. M. W.; Johnson, B.; Chen, W.; Wong, M. W.; Gonzalez, C.; Pople, J. A. *Gaussian 03*, revision B.04; Gaussian, Inc.: Pittsburgh, PA, 2003. (b) Malikin, V. G.; Malkina, O. L.; Eriksson, L. A.; Salahub, D. R. In *Modern Density Functional Theory, A Tool for Chemistry, Seminario*; J. M., Politzer, P., Eds.; Elsevier: New York, 1995. (c) Engels, B.; Eriksson, L. A.; Lunell, S. *Adv. Quantum Chem.* **1997**, *27*, 297. (d) Cancès, M. T.; Mennucci, B.; Tomasi, J. *J. Chem. Phys.* **1997**, *107*, 3032. (e) Mennucci, B.; Tomasi, J. *J. Chem. Phys.* **1997**, *106*, 5151. (f) Mennucci, B.; Cancès, E.; Tomasi, J. *J. Phys. Chem. B* **1997**, *101*, 10506. (g) Tomasi, J.; Mennucci, B.; Cancès, E. *J. Mol. Struct. (THEOCHEM)* **1999**, *464*, 211.

(14) http://jmol.sourceforge.net

(15) (a) Pentz, L.; Thornton, E. R. *J. Am. Chem. Soc.* **1967**, *89*, 6931−6938 and references therein. (b) Washabaugh, M. W.; Jencks, W. P. *Biochemistry* **1988**, *27*, 5044−5053. (c) Krezel, A.; Bal, W. *J. Inorg. Biochem.* **2004**, *98*, 161−166 and references therein.

(16) (a) Gorb, L.; Leszczynski, J**.** *J. Am. Chem. Soc.* **1998**, *120*, 5024. (b) Llano, J.; Eriksson, L. A. *Phys. Chem. Chem. Phys.* **2004**, *6*, 4707−4713.